Optic Nerve Degeneration and Reduced Contrast Sensitivity Due to Folic Acid Deficiency: A Behavioral and Electrophysiological Study in Rhesus Monkeys

Elisa Santandrea,[1] Ilaria Sani,[1,2] Gianpaolo Morbioli,[3] Domenico Multari,[4] Giorgio Marchini,[1] and Leonardo Chelazzi[1,5]

[1]Department of Neuroscience, Biomedicine and Movement Sciences, University of Verona, Verona, Italy
[2]The Rockefeller University, New York, New York, United States
[3]Interdepartmental Centre of Experimental Research Service, University of Verona, Verona, Italy
[4]CVO Fontane, Centro Veterinario Oculistico, Fontane di Villorba, Treviso, Italy
[5]National Institute of Neuroscience, Verona, Italy

Correspondence: Leonardo Chelazzi, Department of Neuroscience, Biomedicine and Movement Sciences, University of Verona, Strada Le Grazie 8, Verona 37134, Italy; leonardo.chelazzi@univr.it.

Submitted: May 31, 2018
Accepted: November 11, 2018

Citation: Santandrea E, Sani I, Morbioli G, Multari D, Marchini G, Chelazzi L. Optic nerve degeneration and reduced contrast sensitivity due to folic acid deficiency: a behavioral and electrophysiological study in rhesus monkeys. 2018;59:6045–6056. https://doi.org/10.1167/iovs.18-24822

Purpose. The purpose of the research was to elucidate the role of folic acid (B_9) deficiency in the development of nutritional optic neuritis and to characterize the neurophysiological consequences of optic nerve degeneration in the cortical visual system.

Methods. A combined behavioral and electrophysiological approach was applied to study luminance contrast sensitivity in two macaque monkeys affected by nutritional optic neuritis and in two healthy monkeys for comparison. For one monkey, a follow-up approach was applied to compare visual performance before onset of optic neuropathy, during the disease, and after treatment.

Results. Optic nerve degeneration developed as a consequence of insufficient dietary intake of folic acid in two exemplars of macaque monkeys. The degeneration resulted in markedly reduced luminance contrast sensitivity as assessed behaviorally. In one monkey, we also measured visual activity in response to varying contrast at the level of single neurons in the cortical visual system and found a striking reduction in contrast sensitivity, as well as a marked increase in the latency of neuronal responses. Prolonged daily folate supplementation resulted in a significant recovery of function.

Conclusions. Folic acid deficiency per se can lead to the development of optic nerve degeneration in otherwise healthy adult animals. The optic nerve degeneration strongly affects contrast sensitivity and leads to a distinct reduction in the strength and velocity of the incoming signal to cortical visual areas of the macaque brain, without directly affecting excitability and functional properties of cortical neurons.

Keywords: folic acid deficiency, optic neuritis, optic nerve demyelination, contrast sensitivity, mid-tier cortical visual areas

Optic neuritis refers by convention to any optic nerve affliction due to demyelination. Although primary demyelinating inflammation in isolation or in association with multiple sclerosis is the most typical cause, other clinical conditions may lead to optic neuritis, notably nutritional deficiencies.[1–3] Fairly uncommon in isolation, nutritional deficiencies are often blended with other causes, like the habitual consumption of toxic substances[2] or specific genetic alterations (e.g., adenosine triphosphate deficiency[4]). Nutritional optic neuritis is generally characterized by bilateral painless reduction in visual acuity that manifests as gradual loss of vision associated with optic atrophy, or sudden loss of vision in the presence of optic disc swelling.[5–9] Optic nerve head appearance can vary from normal to diffusely pale. Patients also may report poor color vision and central/cecocentral scotomas.[7]

Several studies suggested a crucial role of B-complex vitamin deficiencies in nutritional optic neuropathy[10]; in particular, cobalamin (B_{12}) deficiency, commonly related to inborn errors of metabolism, such as in pernicious anemia, has been proven to cause optic neuropathy both in humans and animals.[11–13]

Folic acid (B_9) deficiency also has been proposed as a possible etiological factor for optic neuritis.[5,6] As a confirmation, specific therapy with prolonged daily supplementation of folic acid was demonstrated to produce clinical improvement, eventually leading to a complete recovery from optic neuritis after a long time.[5–9] However, evidence from clinical studies in humans is typically contaminated by the coexistence of multiple etiological factors whose single contribution is therefore very difficult to disentangle. In fact, folic acid–deficient optic neuritis most frequently occurs in patients whose nutritional deficits regard the whole B complex and/or in association with alcohol and/or tobacco intake[5,8,9] or even with a diagnosis of Tobacco-Alcohol Amblyopia[6,7] (TAA), thus impeding a full understanding of the distinct role of folic acid in the development of optic nerve damage. Notably, in some cases of TAA associated with no nutritional deficiencies, substantial recovery from optic neuritis was observed in patients who just

reduced alcohol and tobacco consumption.[14,15] Given controversial evidence for cases of optic neuritis associated with B_9 deficiency in isolation, a major role in nutritional optic nerve damage is conservatively ascribed to other factors usually combined with it, namely B_{12} deficiency and/or alcohol and tobacco abuse. In sum, although available data suggest that folic acid may play a role in the genesis, onset, and development of visual impairments of retinal origin, together with other factors, it is much less clear whether folic acid deficiency per se can be the cause of nutritional optic neuritis.

In this article, we report a behavioral and electrophysiological examination of two cases of optic neuritis in rhesus monkeys (performed in a highly controlled environment), shedding new light on this controversy. Here the disease was attributable to prolonged, unwanted, insufficient dietary intake of folic acid, in the absence of other clinical signs of disease or dysfunction. The present research therefore directly attests to a crucial role of folic acid deficiency in the development of optic nerve disease.

Methods

Animal Model and Training Procedures

Four adult male macaque monkeys (*Macaca mulatta*) were studied in the present research (weight: monkey B = 12 kg; monkey C = 6.5 kg; monkey F = 11 kg; monkey T = 6.5 kg). All monkeys were in good general health, with no clinical history or current clinical signs of infectious or infesting pathologies. A slight chronic increase in the blood level of creatinine (in the range between 2.5 and 2.8 mg/dL), likely reflecting normal aging and minor, well-compensated renal impairment, was detected in monkey B at the time of the second screening (see Fig. 1C and Results).

The animals were housed in the primate area of the Animal Care Facility of the University of Verona (CIRSAL), in conformity with current laws and regulations. The health conditions of animals in the colony were regularly assessed by a veterinary doctor, and the same doctor was responsible for detecting any sign of stress or discomfort. Dedicated personnel took daily care of the animals, cleaning the cages and providing a fully integrated pellet food diet and water. As the pellet food should have contained all necessary nutrients for the monkeys' daily dietary needs (but see Results), food supplementation (e.g., fresh or dry fruit and vegetables) was distributed as a form of environmental enrichment and reward, without systematic nutritional purposes.

The monkeys, engaged in different research projects during the preceding 2 to 10 years, had been previously implanted for single-neuron recording experiments, including with a head-holding device, a scleral eye coil for monitoring eye position[16] and, in the case of monkeys B and F, with a recording chamber over the dorsal portion of Visual area 4 (V4d), as described in detail elsewhere.[17] Before surgery, structural magnetic resonance images of the animals' brains had been obtained with a 1.5-T scanner, whereas the anesthetized monkeys were placed in a stereotaxic apparatus. The images (3-mm-thick coronal slices) had been used to guide placement of the recording chamber over dorsal area V4 on the exposed surface of the prelunate gyrus.[17] In addition, the monkeys had been trained to sit in a primate chair and perform behavioral tasks for research projects pertaining to the study of perception and visual selective attention. They were able to discriminate visual stimuli presented at a certain eccentricity on a computer monitor, while maintaining central fixation; specifically, the monkeys produced a behavioral response based on learned stimulus-response associations. Use of macaque monkeys and research protocols received formal approval by the University of Verona Committee for Animal Research and by the Department for the Veterinary Public Health, Nutrition, and Food Security of the Italian Ministry of Health (D.L. 116/1992, art. 8/9; D.M. 19/2007c, 13/02/2007; and 200/2009c, 11/11/2009). The study was performed in accordance with the guidelines of the EU Directives (86/609/EEC; 2010/63/EU) and the Italian national law (D.L. 116–92, D.L. 26–2014) on the use of animals in scientific research. We confirm full adherence of our research protocols to the ARVO Statement for the Use of Animals in Ophthalmic and Vision Research.

Neuronal Recordings

Extracellular single-unit recordings were obtained from cortical visual area V4d of monkey B and monkey F, while the animals performed an orientation discrimination task involving stimuli presented at different contrast levels (see Methods, Behavioral Assessment). The choice of the target area for recordings was based on several considerations. First, our group has considerable expertise in recording single-neuron activity within area V4d and a good grasp of neuronal properties in this area, which was instrumental to more easily appreciating deviations from normal function. Second, recordings within this cortical region (but not others) were already planned in the authorized protocol running in the laboratory at the time this research was started, which enabled us to obtain relevant data exactly in the critical phase. Finally, we also reasoned that this intermediate processing stage along the ventral cortical visual hierarchy was an ideal candidate for correlating patterns of neuronal activity with the behavioral measures that we obtained by applying the psychophysical method described below, perhaps more so than earlier (e.g., area V1) and later (e.g., IT cortex) stages of the visual pathway.

Recordings were made using transdural, extracellular, tungsten microelectrodes (impedance ~1 MΩ at 1KHz) controlled by a hydraulic microdrive (Micropositioner model 650; Kopf Instruments, Tujunga, CA, USA). Individual spike waveforms were discriminated using an online spike-sorting system (SPS-8701; Signal Processing Systems, Prospect, Australia) and acquired for off-line analysis at 1 KHz on a PC. Concerning the cell-sampling criterion, for all tested monkeys, we applied an identical procedure. First, as we advanced the electrode through the cortical tissue within area V4d, we selected cell spikes characterized by well-defined waveforms, a good signal-to-noise ratio, and a good stability. In most experimental sessions, two neurons could be identified simultaneously and differentiated on the basis of the size and shape of the spike waveform. Receptive field (RF) borders were determined by the minimum response field method[18] and used to place the stimuli in the appropriate location. The selected cells were then probed with a whole set of different visual stimulations (e.g., bars of varying orientation and luminance contrast, including high-contrast stimuli) to qualitatively test their visual responsiveness. Complete recordings from isolated neurons were obtained when they showed at least some response(s) to the tested visual stimuli. However, we also collected data for apparently nonresponsive neurons when they were isolated in the proximity of clearly visually responsive neurons within the same recording session, either if recorded simultaneously or if isolated at slightly higher/lower depth within the same electrode penetration.

Behavioral Assessment

Orientation Discrimination Task. During the experimental sessions, the monkey seated in a primate chair at 57 cm from a cathode ray tube monitor. The task required the animal

Investigative Ophthalmology & Visual Science

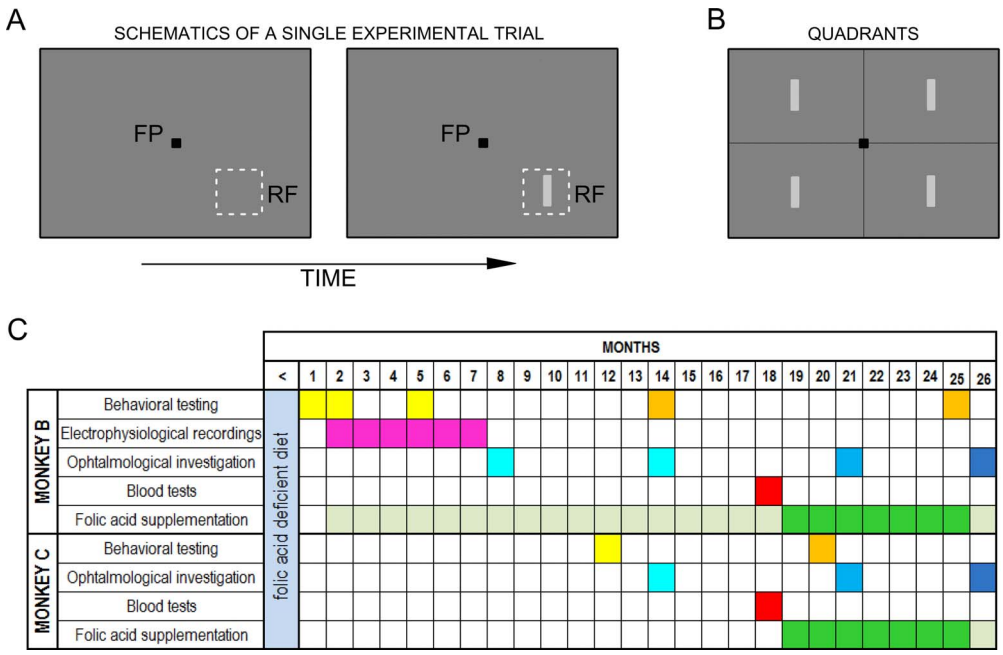

Figure 1. (**A**) Temporal sequence of events in the behavioral task. FP, fixation point; RF, classical receptive field (here indicated by the *dashed square*); the *bar* represents the stimulus to be discriminated. (**B**) Schematics of how single bar stimuli were presented within visual quadrants across the visual field. (**C**) Time line of the critical events in the progression of the study is reported for monkeys B and C (expressed in months from the first screening phase). For behavioral testing, *yellow shading* indicates testing with the orientation discrimination task, whereas *orange shading* indicates CS tests (involving assessment of CS in all quadrants of the visual field). For ophthalmological investigations, in an initial phase of the study, only a standard clinical assessment under general anesthesia was performed (*cyan*); subsequently, we also acquired ERG data (*light blue*) and digital camera photos of the retina (*light blue* and *blue*). Folic acid supplementation was administered by protocol for a total of 7 months (*green*); *light green* shading indicates epochs in which correct daily intake of folic acid was also guaranteed by appropriate food pellet delivery (see text for details).

to discriminate the orientation of an achromatic bar stimulus (2.2×0.3 deg of visual angle) by turning a lever either to the right or to the left. A specific lever response was associated with each of four possible orientations of the stimulus (vertical, horizontal, tilted 45° right, and tilted 45° left), and the associations were learned by the animals during early phases of the training process. Two nonorthogonal orientations, requiring opposite lever responses, were selected for each recording session. Because most neurons in area V4d show substantial selectivity for orientation,[19] we selected one stimulus for being of the preferred orientation for the neuron under study, and the other for being of a suboptimal (nonorthogonal) orientation for the same neuron, but still able to evoke a significant visual response. The bar stimuli were presented at seven luminance contrast levels (2.5%, 5%, 10%, 20%, 40%, 80%, 94% Michelson contrast) on a constant background (2.5 cd/m^2). On each trial, the monkey was required to maintain fixation onto a central fixation spot (black square, 0.3×0.3 deg) and to discriminate the orientation of a bar stimulus inside the RF of the recorded neuron (Fig. 1A). Central fixation was ensured by recording position of one eye by means of the scleral search coil method[20] (sampling rate: 250 Hz). The monkey had a maximum of 1500 ms to produce the response. After 500 ms, the stimulus disappeared; if the response was given before, the stimulus disappeared at the time of response. The monkey was rewarded with fruit juice for each correct response. While the animals were performing the task, both behavioral responses and single-cell spiking activity were recorded.

Contrast Sensitivity Assessment. Contrast sensitivity was assessed by means of a highly reliable behavioral test collecting lever responses of the animals to oriented bar stimuli. The test was a variant of the previously illustrated task. In successive blocks of trials, single bar stimuli at varying luminance contrasts were presented in all the four quadrants of the visual field to assess possible differences in contrast sensitivity (Fig. 1B). The contrast levels used in the present study covered a broad range of possible contrasts (2.5%, 5%, 10%, 20%, 30%, 40%, 60%, 80%, 94% Michelson contrast). However, different set sizes (five, seven, or nine contrast levels) were used to accommodate for the visual impairment in some of the tested animals; for example, in the case of a strong visual impairment, we decided to exclude the lowest (or the lower two) contrast level(s), to avoid the animal experiencing too many "invisible" stimuli, which will cause excessive distress and ultimately will turn into unwillingness to collaborate in the test. In all cases, contrasts within the selected range were chosen randomly on each trial. Accuracy (percentage of correct responses) was measured to describe the performance of the monkeys. In monkey B, contrast sensitivity assessments were repeated periodically to follow up the development, and possible recovery, of the visual deficits.

Data Analyses

Fitting Procedures. To obtain reliable estimates of contrast sensitivity both at the behavioral and neuronal levels, both psychometric functions and single-neuron contrast response functions (CRFs) were determined by using a nonweighted least-square fitting procedure (Curve Finder Tool, Matlab; MathWorks, Natick, MA, USA). In the former case, we applied a best-fitting procedure to the average behavioral accuracy of the animal as a function of stimulus contrast; in the latter case, for each recorded neuron, we applied the fitting procedure to the mean firing rate calculated in a temporal window from 50 to 200 ms

after the onset of the visual stimulus, separately for the preferred and unpreferred orientation of the stimulus. We fitted a Naka-Rushton function, traditionally used in the neurophysiological literature to describe the sigmoidal patterns of response to contrast in cortical visual neurons[21]: $Accuracy\ (or\ Response) = \frac{R_{max} * C^n}{C_{50}^n + C^n} + R_0$, where R_{max} is the maximal accuracy (or maximal firing rate of the neuron), R_0 is the estimated baseline performance (or the undriven activity of the neuron), C_{50} is the semisaturation contrast, that is, the contrast value corresponding to half of the maximal accuracy (or response rate of the neuron), and n represents the slope of the curve as measured at the semisaturation contrast. For psychometric curves, we then calculated *contrast threshold* (CT), as the contrast value corresponding to the 75% of correct responses, as mathematically derived from the fitted function, and *contrast sensitivity* (CS), as the reciprocal of CT (e.g., Ref. 22). For single-neuron CRFs, data recorded with the preferred and unpreferred orientation of the stimulus were analyzed separately, thus obtaining two fitted CRFs for each neuron. We evaluated the goodness of fit by calculating the R-square value (1-SSE/SST, where SSE is the Sum of Squares Error, SST is Sum of Squares Totals); results were described and further analyzed only for well-fitted cells (R-square > 0.5), that is, 87.82% and 78.02% of the total CRFs measured for the preferred and unpreferred orientation of the stimulus, respectively. We focused on the semisaturation contrast, C_{50}, traditionally taken to represent the neuronal CS.

Neuronal Latency. Latency of the neuronal response for each luminance contrast level was calculated separately for the preferred and unpreferred stimulus orientation. Operationally, we constructed a peri-stimulus time-histogram (PSTH) and smoothed it with a Gaussian filter ($\sigma = 8$ ms); we then defined and calculated latency as time to half the peak of the response waveform.[23] Latency was calculated only for PSTHs leading to a peak firing level exceeding the baseline activity by more than 2 SDs, that is, where visual response was strong enough to derive a reliable measure of response latency.[23,24] If a reliable measure of latency was not obtained for all conditions tested in a given neuron, the cell was discarded from statistical analyses. Overall, for this reason, 7.7% of the neurons had to be excluded for monkey F (13 of 168). In the case of monkey B, we could reliably measure latency only for the three higher contrasts of the stimulus, as no reliable visual response was detected for lower contrasts. Therefore, the inclusion criterion was applied only to data collected for these three contrast levels; as a result, we discarded 22.5% of the recorded neurons (16 of 71).

Results

Loss of Contrast Sensitivity

We began to be concerned with the visual sensitivity of our monkeys during the training phase of a research project concerning the interplay between visual signals related to the encoding of luminance contrast and cognitive signals related to spatially directed attention.[25,26] After substantial practice and learning with an orientation discrimination task, in which the monkeys were required to discriminate the orientation of a bar stimulus shown at varying luminance contrast levels (see Methods), the behavioral performance of one of the monkeys under training (monkey B) started to deteriorate without any apparent reason (as explained in more details in what follows). The monkey had already reached a good level of performance at the task, was apparently in good health and maintained a collaborative attitude during the training sessions. We therefore began to investigate the possible reasons underlying the measured worsening in performance, by means of behavioral and electrophysiological testing, clinical and ophthalmological assessment, and a thorough examination of the whole nonhuman primate colony in our facility. In what follows, we report on the systematic research project that stemmed from this initial observation, starting from an initial assessment of CS in monkey B (see Fig. 1C). It is important to note that what is reported here as a sort of baseline performance (first screening) in relation to the subsequent manifestation of a clear pathological condition, was in fact already suboptimal, but not so compromised as to lead to significant concerns on our part.

In a first screening phase (covering 17 testing sessions), behavioral data were collected from monkey B, while it was performing an orientation discrimination task on achromatic bar stimuli varying in luminance contrast (see Methods). Accuracy in performance was calculated as the percentage of correct responses separately for each contrast level (and each tested orientation) of the stimulus. To measure CS, data were then fitted by a Naka-Rushton equation to obtain the psychometric function of the animal and to derive the parameters of interest (see Methods). As measured via the application of fitting procedures on average accuracy data collected during the first screening phase, for this animal, CT was at 14.1% Michelson contrast, corresponding to a CS of 7.1 (0.8513 log units [LU]).

In a period of 4 months from the first screening, monkey B progressively developed a deficit of the visual function (i.e., a strong reduction in CS). Figure 2A depicts percentage of correct discriminations for monkey B in the first screening and in two subsequent phases, namely after 1 month (second screening; comprising 13 testing sessions) and after 4 months (third screening; comprising 20 testing sessions) (see Fig. 1C). A repeated-measures ANOVA was performed on the collected data with the factors Screening (three subsequent screening phases) and Contrast (seven contrast levels). Overall, as expected, performance was significantly modulated by the level of contrast of the stimulus to be discriminated ($F_{6,329} = 273.66$, $P << 0.001$), with the percentage of correct responses increasing as stimulus contrast increased. Crucially, we could also assess a strong, general worsening in performance across subsequent screening phases ($F_{2,329} = 89.81$, $P << 0.001$). The observed decrease in performance was not homogeneous across contrast levels, nor across subsequent screenings, as evidenced by a statistically significant interaction between the two considered factors ($F_{12,329} = 12.62$, $P << 0.001$). Because no change in performance was expected for the lower, near-threshold contrast levels (2.5% and 5% contrast, for which accuracy was already at chance in the very first screening phase), we applied pairwise statistical comparisons (Bonferroni corrected, unpaired, two-tailed *t*-tests) to compare performance across subsequent screening phases only to above-threshold contrast levels ($\geq$10% Michelson contrast). As a result, we could confirm a strong reduction in performance for intermediate (but not high) contrast levels from the first to the second testing phase (screening 1 vs. 2; $P < 0.05$, Bonferroni corrected; Fig. 2A, black asterisks), and only a trend for a significant reduction in accuracy of responses to stimuli displayed at 20% contrast when comparing data collected in the second versus third screening phase (Fig. 2A, gray asterisk). In all cases, therefore, the discrimination accuracy remained quite high and almost stable for the highest contrast levels, in the saturating portion of the psychometric curve, while becoming progressively compromised for intermediate contrast levels, within the dynamic range of the psychometric curve (Fig. 2A). As established by applying fitting procedures to average accuracy data collected during the third screening,

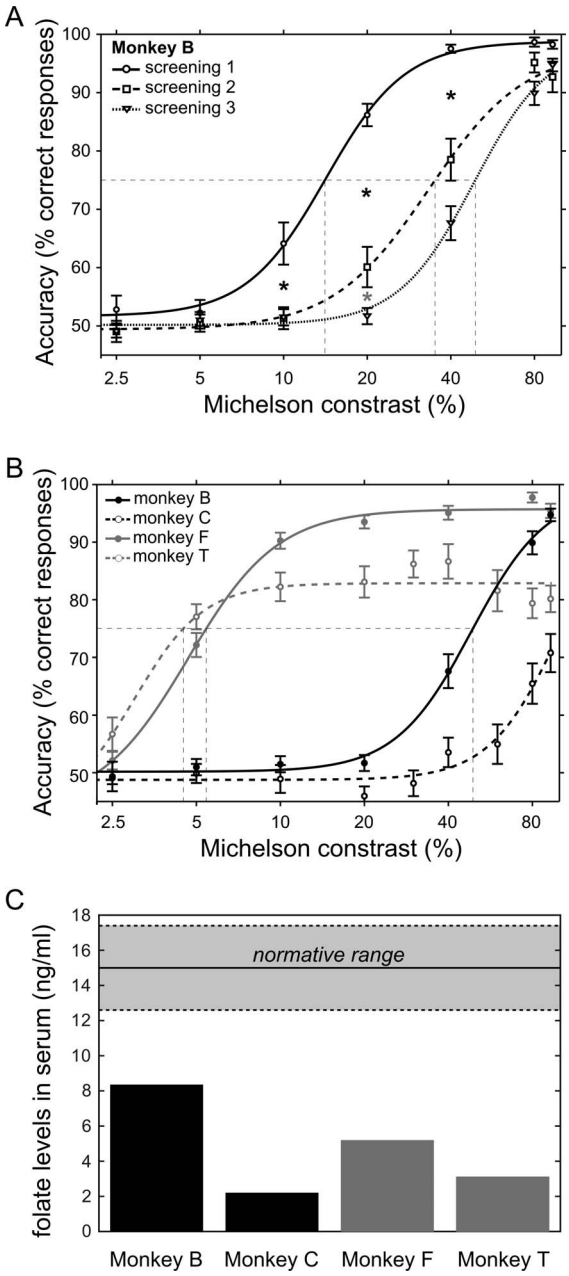

Figure 2. Psychometric curves for contrast. (**A**) Development of a deficit in CS in monkey B. Accuracy (% of correct responses; mean ± SEM) at the orientation discrimination task is reported as a function of stimulus contrast in three subsequent screening phases (see text). Psychometric curves were obtained by applying fitting procedures (see Methods); *thin dashed lines* indicate CT as mathematically derived from each fitted curve. (**B**) Comparison of four animals in the colony. Psychometric curves for contrast were estimated in four animals of the colony (conventions as in [**A**]). Although two of them (monkeys B and C) showed a CS deficit, the other two (monkeys F and T) were unimpaired. Note that the *black solid curve* for monkey B depicted here corresponds to that reported in (**A**) (third screening). (**C**) Folate levels in the serum are reported for all monkeys (*bar graph*), together with an indication of the normative range for rhesus monkeys.

CT increased to 49% Michelson contrast, corresponding to a CS of 2.85 (0.4548 LU).

To check for the possible presence of a similar deficit of the visual function, three additional exemplars in the colony were subsequently tested using the same orientation discrimination task. A strong deficit in CS was found in monkey C (Fig. 2B, black dashed line), which was evidently impaired in the discrimination task even for stimuli of high-contrast level; for example, performance was not reliably different from chance level even for a stimulus presented at 60% Michelson contrast (two-tailed, one-sample *t*-test; $P = 0.169$). Conversely, CS was relatively normal in monkey F and in monkey T (Fig. 2B, gray lines), and well in line with performance profiles reported in the literature for macaque monkeys (e.g., Refs. 21, 24–26). As before, we obtained the psychometric function for the three additional animals by fitting a Naka-Rushton equation to their average accuracy data. For monkey C, it was not even possible to estimate the CT, because performance did not reach the 75% of correct discriminations even for the maximum contrast level (the interpolated performance value at 100% contrast was 74.19%). For monkey F and monkey T, CT was 5.43 and 4.49% Michelson contrast, corresponding to a CS equal to 18.43 (1.2655 LU) and 22.25 (1.3473 LU), respectively, well in the normal CS range for macaque monkeys (e.g., Ref. 27).

Ophthalmological Investigation

Following ophthalmological examination under general anesthesia, optic neuritis was ascertained in monkeys B and C (but not in monkeys F and T). Optic atrophy was revealed by a diffuse and bilateral pallor of the optic nerve head (Fig. 3, left panels). Optic atrophy was not accompanied by optic disc swelling, suggesting the absence of any ongoing inflammatory process. No sign of pathology was discovered at the level of the retina, the vitreous, the lens, or the cornea. Notably, ERG testing following a dark-adaptation protocol (administered after full pupil dilation and 20 minutes of dark adaptation; under general anesthesia) confirmed normal intraretinal function in all four exemplars in the colony.

We then conducted a careful clinical investigation to identify the causes of the disease, including the assessment of blood levels of different vitamins (notably, folate and cobalamine) and the examination of dietary intake and environmental exposure to potential toxic substances (as explained in more details in what follows). This systematic investigation led to ascertain that the optic neuritis had developed as a result of a nutritional folic acid deficiency. Folate levels in the serum corresponded to 8.34 and 2.19 ng/mL in monkeys B and C, respectively, and to 5.18 and 3.1 ng/mL in monkeys F and T, respectively (Fig. 2C). (A slightly higher folate level in monkey B might be attributed to the fact that, during the time in which the described investigations were conducted, pellet food supplied to monkey B was substituted with a new one, with lower protein content in consideration of the slight increase in the blood level of creatinine [see Methods]. Incidentally, this new pellet food was also verified a posteriori to guarantee an appropriate daily intake of folic acid.) All these values were well below the normative range for rhesus monkeys[28,29] (15.0 ± 2.4 ng/mL; Fig. 2C). In fact, and to our astonishment, the folate concentration in the pellet food (which the monkeys had consumed at least during the past 5 years) was found to be insufficient for the macaque nutritional requirements, as confirmed by ad hoc chemical analyses. Specifically, although a sufficient daily intake of folic acid for rhesus monkeys has been estimated to be at least 1.5 mg/kg of dietary dry matter[30] the actual concentration in the pellet food delivered to the monkeys was 0.84 ± 0.06 mg/kg of dry matter. This resulted in a chronic deficiency of folic acid, which in two of the four monkeys led to an overt pathology and visual deficit. Known potential concurrent etiological factors were safely rejected. First, as mentioned above, no clinical history or current clinical signs of infectious or infesting pathologies were detected, as

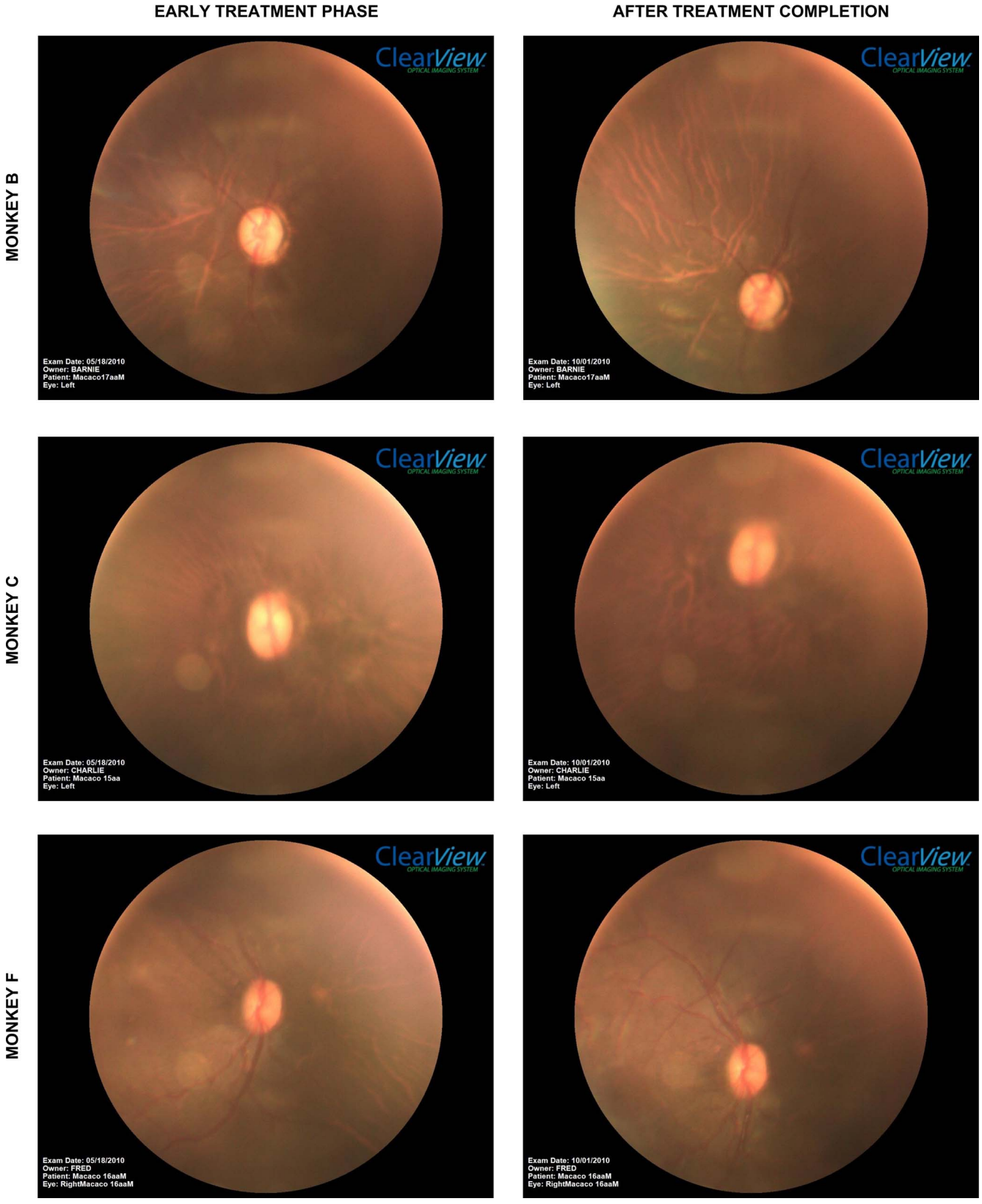

FIGURE 3. Retinal images obtained at an initial stage of the pharmacological treatment and after treatment completion. Retinal images obtained with a digital retina camera (ClearView, Optic Imaging System; Kruuse, Langeskov, Denmark) showing the optic nerve head status are reported for monkeys B and C (and for monkey F for comparison); images were acquired soon after the time of the first diagnosis (*left*; see Fig. 1) and after completion of folic acid supplementation (*right*; note that retinal images obtained from the same eye are shown for the two time epochs). Please note that, at the exact time of the first diagnosis, when the ophthalmological assessment revealed a diffuse pallor of the optic nerve head, we did not have access to this technique. However interesting for scientific purposes to photographically document the clinical condition before the start of any treatment, it would have been unethical to procrastinate the latter because of technical reasons. Thus, images shown on the *left* were taken after 2 months from the start of the pharmacological treatment; at this time, pallor of the optic nerve was still evident for monkeys B and C.

Investigative Ophthalmology & Visual Science

certified by the local veterinary doctor, also following blood examination. Second, no deficit in the serum level of cobalamin was detected. Finally, a series of common toxic factors[3] (e.g., methanol, ethambutol) could also be excluded, after careful examination of chemical compounds present in products of normal use in the animal facility (e.g., cleaning products for animal housing rooms, litter). Although no clear contribution could be attributed to other typical causes of the disease, it remains to be established which factors (likely to be sought in the individual genetic profile) might have had an influence on the development of the overt pathology only in two of four exemplars with a severe nutritional deficiency, a problem that stands as a pervasive issue in all modern medicine. In fact, following comparable exposure of a population of individuals to a given noxa or pathogen factor, the incidence of the overt disease is typically well below 100% in the given population. The reasons for this reside in a multitude of potentially uncontrolled factors related primarily to the individual profile (e.g., genetic and metabolic traits), which might act either as contributing cofactors for the insurgence of the overt pathology or, on the contrary, as protecting factors. In addition, another aspect to take into consideration is the exact timing of insurgence of the disease; we started folate compensation (see Results, Recovery After Folic Acid Integration) when the overt deficit was diagnosed in two of four exemplars in our nonhuman primate colony, but it remains possible that the other animals would have developed the deficit subsequently in the absence of any treatment. Regardless of these considerations, our data demonstrate that a severe folic acid deficiency might be a stand-alone inducing factor for the development of optic neuritis, without being an absolute determinant of its overt manifestation.

Contrast Sensitivity Assessment

To better characterize the visual deficit in the two monkeys affected by optic neuritis, we performed a systematic assessment of CS (see Methods). Specifically, accuracy at the orientation discrimination task was measured for single stimuli of varying luminance contrast presented in the four quadrants of the visual field in separate blocks (at 4° of eccentricity) (see Methods for additional details). Monkey B showed a nonuniform deficit in CS across the visual field, with relatively preserved visual function in the right hemifield and especially in the lower right quadrant (Fig. 4A). Monkey C, instead, showed a homogeneous and marked deficit across all quadrants (Fig. 4B).

Electrophysiological Study

We set up an electrophysiological study to investigate the effects of optic nerve degeneration at the level of the cortical visual system. Data were collected from a visually impaired animal (monkey B) and from an unimpaired animal (monkey F) for comparison. (Electrophysiological data were additionally recorded in the other healthy animal, monkey T. Measured patterns of activity in V4d neurons were fully consistent with those reported for monkey F,[25,26] as well as with the literature (e.g., see Refs. 21, 24), and will not be shown here for the sake of brevity. Conversely, we did not conduct electrophysiological experiments in monkey C because, due to the gravity of the reduction in CS, this animal had impaired performance at the task for most low and intermediate contrast levels, thus making a systematic electrophysiological investigation unfeasible.) We recorded the activity of single neurons from area V4d, an intermediate node along the ventral stream of the cortical visual system[19,31,32] while the monkeys performed the orientation discrimination task, as used during the initial screening phase (see Methods). Following a preliminary evaluation on the quality of recordings, assessing signal stability within the recording session and a congruous number of repetitions (≥12) for each experimental condition, we gathered a dataset of 171 cells for monkey B and 217 cells for monkey F, respectively.

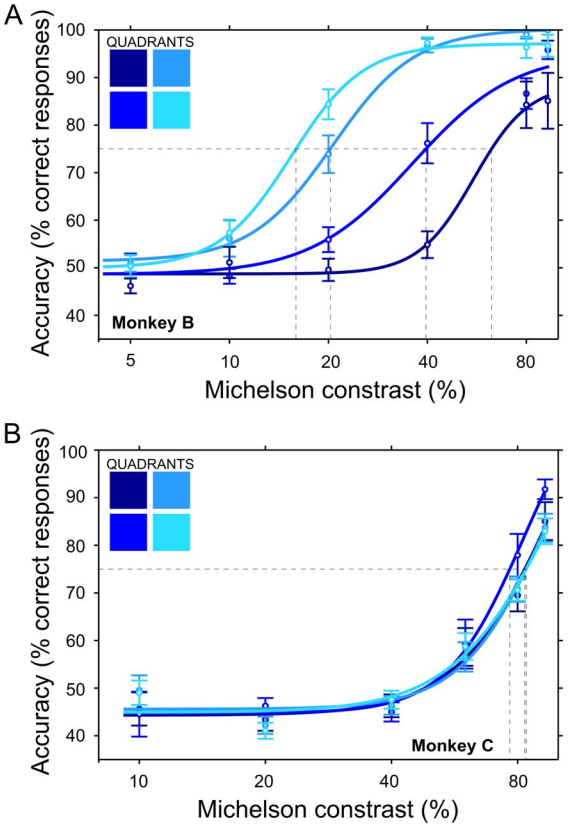

FIGURE 4. Contrast sensitivity assessment. (**A**) Psychometric curves for contrast (conventions as in Figs. 2A, 2B) are reported for monkey B, separately for stimuli presented in the four quadrants (see color legend). CT (in % Michelson Contrast) values and corresponding CS values were calculated separately for each quadrant and were equal to the following: CT = 39.6076, CS = 0.4022 LU (*lower left quadrant*, *blue*); CT = 62.7356, CS = 0.2025 LU (*upper left quadrant*, *dark blue*); CT = 20.26065, CS = 0.6933 LU (*upper right quadrant*, *azure*); CT = 15.9302, CS = 0.7978 LU (*lower right quadrant*, *cyan*). (**B**) *Psychometric curves* for contrast as measured in the four quadrants of the visual field (see color legend) are reported for monkey C. Again, CT and CS values were calculated separately for each quadrant and were equal to the following: CT = 76.61275, CS = 0.1157 LU (*lower left quadrant, blue*); CT = 83.203, CS = 0.0799 LU (*upper left quadrant*, *dark blue*); CT = 83.8234, CS = 0.0766 LU (*upper right quadrant*, *azure*); CT = 83.8559, CS = 0.0765 LU (*lower right quadrant*, *cyan*).

To begin with, we evaluated single-cell *visual responsiveness* by conducting a series of paired *t*-tests to compare the average firing rate of the neuron following stimulus presentation (50–200 ms post stimulus onset) against baseline activity (in a 150-ms window preceding stimulus onset) in each experimental condition. We then calculated a Responsiveness Index (RI) for each neuron, corresponding to the cumulative number of visual responses that were significantly different from undriven activity (two-tailed, paired *t*-test; $P < 0.05$, Bonferroni corrected). The index value could range from 0 to 14, corresponding to the total number of experimental conditions (seven luminance contrast levels × two orientations). A striking difference emerged in the proportion of *nonresponsive* cells (RI = 0), which was more than doubled in

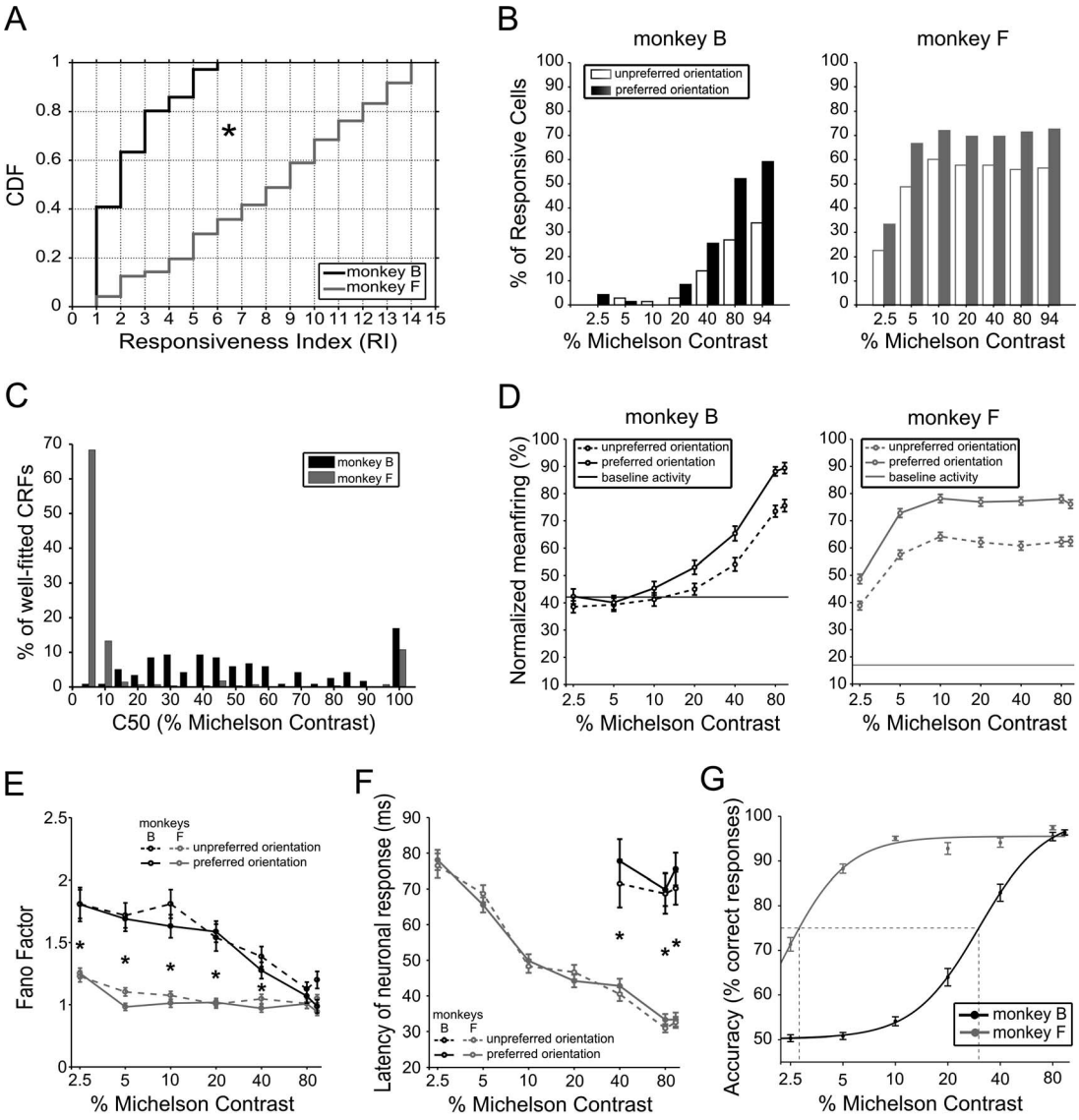

Figure 5. Neurophysiological assessment of CS impairment. (**A**) Cumulative distribution of RI (see text) for responsive cells from monkey B ($n = 71$, in *black*) and monkey F ($n = 168$, in *gray*). (**B**) Percentage of visually responsive cells as a function of stimulus contrast and orientation for monkeys B (*left*) and F (*right*). (**C**) Distributions of C_{50} for well-fitted CRFs of visually responsive cells are shown for monkeys B (*black*) and F (*gray*). Although C_{50} clustered around very low contrast for monkey F, reflecting high-CS in the population of recorded neurons, it was distributed along the entire contrast range for CRFs recorded in monkey B. (**D**) Normalized average firing rate of the population of visually responsive neurons recorded in monkeys B (*left panel*, in *black*) and F (*right panel*, in *gray*). Population activity (mean ± SEM) is shown separately for the preferred (*solid lines*) and unpreferred (*dashed lines*) orientation of the stimulus, together with baseline activity (*horizontal dotted lines*). (**E**) Average across-trial variability in the activity of the population of visual responsive neurons recorded in monkeys B (in *black*) and F (in *gray*). Average Fano Factor is shown as a function of stimulus contrast and orientation (see text for details). (**F**) Neuronal response latency is shown as a function of stimulus contrast and orientation for monkey F cells ($n = 155$; in *gray*) and monkey B cells ($n = 55$; in *black*) (see Methods). (**G**) Psychometric curves for contrast (conventions as in Figs. 2A, 2B) measured for monkey B (*black*) and F (*gray*) during the neuronal recording sessions.

the unhealthy animal (monkey B: 58.5%, 100 of 171 cells) with respect to the control (monkey F: 22.5%, 49 of 217 cells), suggesting a possible reduction in neural activity at the level of area V4 in monkey B due to the impoverished signal ascending through the damaged optic nerve to the cortical visual system.

Subsequent analyses focused on *responsive cells* (71 neurons in monkey B and 168 neurons in monkey F), that is, those cells showing at least one significant visual response (RI >0). The average RI for responsive neurons in monkey B (RI = 2.32 ± 0.18 SEM) was significantly lower than that measured for responsive neurons in monkey F (RI = 8.15 ± 0.30 SEM; two-tailed, unpaired *t*-test, $P << 0.001$). In addition, while RI was distributed across the whole range of values for monkey F neurons, it assumed values between 1 and 6 for monkey B neurons, resulting in a significant difference in cumulative distributions (Kolmogorov-Smirnov test [kstest] = 0.6742, $P << 0.001$; Fig. 5A). In sum, visually driven activity of cells in monkey B was strongly reduced with respect to that assessed in a healthy monkey.

To verify whether reduced V4 activity in monkey B paralleled the behavioral impairment in CS (Fig. 2A), we calculated the percentage of cells showing a significant visual response separately for each luminance contrast level of the stimulus. The distribution of significant responses across contrasts was significantly different in the two monkeys (Fig. 5B), as assessed both for stimuli of the preferred and

unpreferred orientation (both kstest > 0.85; both $P < 0.01$). In monkey F, a high percentage of cells was activated by each contrast level, with a reduction in responsiveness only for the lowest contrast, which was likely below threshold for most of the neurons. Strikingly, in monkey B, we instead observed a considerable percentage of significant visually evoked responses only for stimuli at the highest contrast levels (80%–94% Michelson contrast), whereas this percentage already halved for stimuli at 40% Michelson contrast and was negligible for stimuli at lower contrasts.

Using best-fitting procedures, we quantitatively described neuronal behavior as a function of contrast on a cell-by-cell basis, and directly compared data from the two animals. We determined single-neuron CRFs by fitting the Naka-Rushton function to each neuron's mean firing rate and examined the parameter C_{50}, that is, a measure of neuronal CS[21] (see Methods). Because no difference emerged for C_{50} across stimulus orientations (two-tailed, unpaired *t*-test; $P = 0.2519$ and $P = 0.5040$ for monkey B and F, respectively), results were considered together. The C50 distributions for neurons recorded in the two monkeys were significantly different (two-tailed, unpaired kstest, $P << 0.001$; Fig. 5C), with average C_{50} being significantly higher (52 ± 2.6) for monkey B than for monkey F (16.3 ± 2.9; two-tailed, unpaired *t*-test, $P << 0.001$). Therefore, a strong deficit in CS for monkey B was confirmed at the single-cell level, as compared with the healthy pattern measured in monkey F, as well as with normative data in the literature (e.g., see Refs. 25, 33).

Single-cell results were consistent with a different pattern of response to contrast at the neuronal population level. Figure 5D represents the normalized firing of the neurons recorded in the two monkeys as a function of stimulus contrast. In monkey F, the visually evoked activity of the neurons is already above baseline for a stimulus at 2.5% Michelson contrast and then steadily increases for higher contrasts values, reaching a plateau already at 10% Michelson contrast (right panel). Conversely, the visually evoked activity of neurons in monkey B is reduced or totally abolished for low to medium contrast levels (up to 20%) and is preserved only for high-contrast levels (left panel). Importantly, this difference did not reflect any sign of dysfunction at the level of V4 neurons in monkey B, as maximal firing level of the neurons was comparable between neurons from the two monkeys (two-tailed, unpaired *t*-test, $P = 0.0830$; average maximal firing in spikes/second ± SEM corresponded to 52.2 ± 2.6 and 46.8 ± 1.7 for monkeys B and F, respectively). Rather, decreased activity in V4 reflected a reduced input to this area that ultimately originated from the optic nerve damage.

In addition to the average spiking activity of neurons, we compared trial-to-trial variability in the spike trains recorded in the two animals for each experimental condition, as indexed by the Fano Factor, or the ratio of the across-trial variance in the spike count measured in the considered temporal window (50–200 ms after the onset of the stimulus) divided by the average spike count in the same temporal window (e.g., Ref. 34). For each of the two animals, we calculated the Fano Factor separately for each contrast level of the stimulus, as well as for preferred and unpreferred stimulus orientations (Fig. 5E), and performed a 2-way ANOVA with the factors contrast and orientation. In monkey F, across-trial variability in neural activity decreased as contrast increased ($F_{6,2310} = 11.79$, $P << 0.001$) and was overall slightly lower for the preferred versus unpreferred stimulus orientation ($F_{1,2310} = 6.08$, $P = 0.0137$), in keeping with the idea that the strength of the incoming visual drive predicts the amplitude of the stimulus-driven reduction in the response variability of neurons (e.g., Ref. 34). The same pattern of results was observed in relation to contrast for monkey B, for which again we observed a statistically significant reduction in across-trial variability with increasing contrast ($F_{6,966} = 21.44$, $P << 0.001$). Critically, we also observed a substantial difference in the pattern of variability measured across the two monkeys, as confirmed by the results of a series of unpaired, two-tailed *t*-tests directly comparing the Fano Factor values separately for each experimental condition ($P < 0.05$, Bonferroni corrected; see Fig. 5E). Interestingly, although the Fano Factor for responses to high-contrast stimuli was comparable for neurons recorded from the two monkeys, a higher level of variability was measured for responses to low and intermediate contrast levels in neurons recorded from monkey B, consistent with a substantial reduction in the strength of the incoming visual drive.

We also calculated the latency of neuronal responses, separately for each experimental condition, and performed a 2-way ANOVA with the factors contrast and orientation. In line with previous results,[23–26,35,36] in monkey F we observed a significant decrease in the neuronal latency of response as stimulus contrast increases ($F_{6,2156} = 130.28$, $P << 0.001$) (see Fig. 5F). For monkey B, we could reliably measure latency only for the three highest contrasts (40%, 80%, and 94%). A similar 2-way ANOVA yielded nonsignificant results, as might be expected. Most interestingly, latency of the response to each of the three highest contrast levels was remarkably longer in monkey B with respect to monkey F for both stimulus orientations (unpaired, two-tailed *t*-tests, $P << 0.01$, Bonferroni corrected) (see Fig. 5F). This pattern of results demonstrates that not only visually driven responses were weaker in monkey B with respect to a healthy control monkey, but also that neuronal responses in monkey B were substantially delayed, likely reflecting reduced propagation velocity along the optic nerve due to demyelination (see Discussion).

To establish a direct parallel between neuronal activity and behavior, we finally analyzed performance of the two animals as a function of the stimulus contrast, during the same recording sessions that yielded the electrophysiological data (Fig. 5G) and ascertained that the pattern of accuracy in behavioral responses was perfectly compatible with that of neuronal visually evoked activity (Fig. 5D).

Recovery After Folic Acid Integration

First, pellet food delivered to all monkeys was substituted to ensure correct daily intake of folic acid. (As explained previously, for reasons independent from the present research, pellet food supplied to monkey B had been previously substituted with a new one, incidentally ensuring appropriate daily intake of folic acid. In consideration of this point, folic acid supplementation in monkey B might be considered to have lasted longer than the considered 7 months [see light green shading in Fig. 1]. Although this aspect is important to be taken into consideration, it will be inappropriate to consider the daily intake provided by the new pellet food as a reasonable treatment for a severe deficiency, both in terms of dose and intake method. In consideration of this aspect, we do not draw any conclusion about the exact protocol of pharmacological intervention [dose, length, intake method], which might be appropriate in similar conditions; rather, we focus on theoretical conclusions about a significant stand-alone role of folic acid deficiency in the development of optic neuritis.) In addition, and more critically, a specific integration therapy was immediately started after we realized that all monkeys in the colony had been exposed to insufficient folic acid in the diet for a prolonged period. We administered 7 mg/d of folic acid via intramuscular injection for 10 days and then started an oral supplementation of 5 mg/d for the following 7 months.

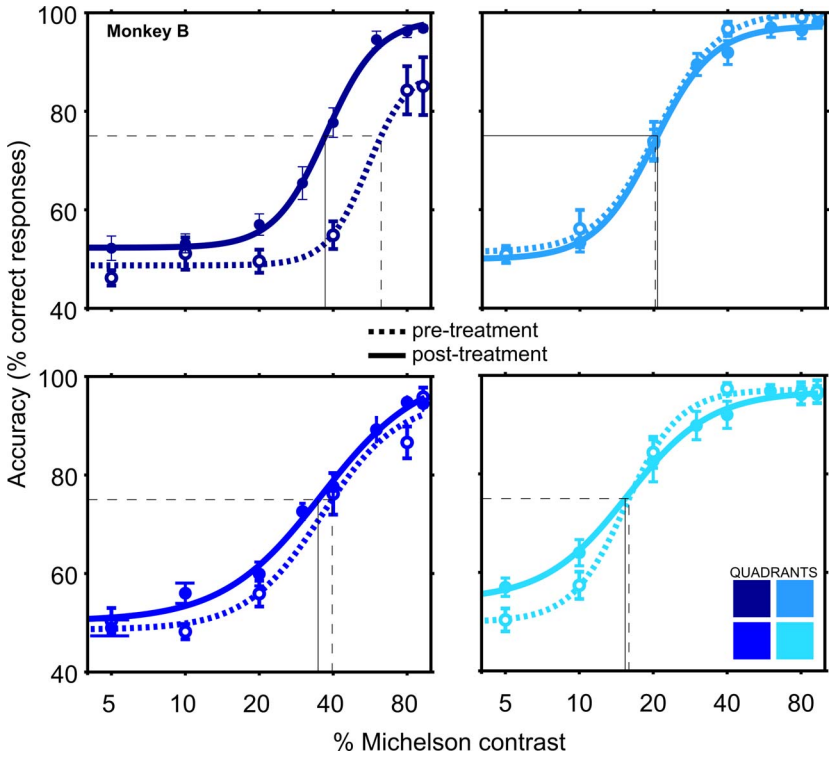

FIGURE 6. Recovery in contrast sensitivity after folic acid therapy in monkey B. The four panels depict accuracy (mean ± SEM) as a function of contrast, separately for each quadrant. Psychometric curves are shown for two CS assessments (see Fig. 1). Results from the first assessment (*dashed lines*) were already reported in Figure 4A together with CT and CS values for each quadrant, and are reported again here for the sake of comparison. Results from the second assessment, which followed 7 months of folate supplementation, are reported with *solid lines. Dotted* and *solid thin lines* indicate CTs before and after the therapy was supplied, respectively, bringing out a clear recovery for the two quadrants originally affected by a stronger deficit (*upper* and *lower left*). CT (in % Michelson Contrast) and CS values for the second assessment corresponded to the following: CT = 34.7076, CS = 0.4596 LU (*lower left quadrant*, *blue*); CT = 37.0777, CS = 0.4209 LU (*upper left quadrant*, *dark blue*); CT = 20.7056, CS = 0.6839 LU (*upper right quadrant*, *azure*); and CT = 15.37485, CS = 0.8132 LU (*lower right quadrant*, *cyan*).

After 7 months of daily folic acid supplementation, clinical investigation revealed partial recovery, as assessed by a reduced pallor of the optic nerve head in both afflicted monkeys (Fig. 3, right panels). We consequently performed a new behavioral test in monkey B and ascertained a significant increase in accuracy at the orientation discrimination task, especially evident in the most severely affected quadrants. Figure 6 reports the results of two CS assessments, performed 11 months apart, separately for each visual quadrant (see Fig. 1). Psychometric curves obtained during the second assessment (solid lines), which followed treatment completion, are shown together with those obtained in a first assessment (dashed lines; see Fig. 4A) for the sake of comparison. A clear, albeit partial, recovery was evident for the two quadrants originally affected by a stronger deficit (upper and lower left), as reflected in considerable changes in CTs (dotted and solid thin lines for pre- and posttherapy assessments, respectively) measured for visual stimulation in those quadrants (Fig. 6). This result unequivocally demonstrates the crucial role of folic acid in the onset of, and recovery from, optic neuritis.

DISCUSSION

Owing to a highly controlled environment and a clear anamnestic framework, which are not easily available in standard clinical studies in humans, the present research provides the first unequivocal demonstration of a distinctive role of folic acid deficiency in the development of optic neuritis in primates. New to the field, besides behavioral testing and the standard ophthalmological examination, we obtained a systematic electrophysiological characterization of the neuronal correlates of the disease at the level of the cortical visual system. With the latter approach, we were able to describe reduced, more variable, and delayed neuronal responses in a mid-tier node of the cortical visual system, likely reflecting inefficient transmission of the preserved retinal input through the demyelinated optic nerve fibers.

In more detail, in the present article, we reported two cases of nutritional optic neuritis in rhesus monkeys that were clearly attributable to a prolonged insufficient dietary intake of folic acid, in the absence of other relevant nutritional deficiencies, including of cobalamin,[11–13] and in the absence of other clinical signs of disease or dysfunction. Given that our monkeys lived and were handled in a highly controlled environment, a number of potential etiological factors, such as exposure to toxic substances or the habitual consumption of substances of abuse, could be safely excluded as contributing causes. In addition, after systematic folic acid supplementation, a recovery was evident both in optic nerve appearance as well as in visual sensitivity, thus providing a strong ex adiuvantibus confirmation of the crucial role of folic acid deficiency per se in the development of optic nerve disease. It is important to underline that the observed recovery of visual function has to be considered partial, rather than complete. This might be because myelin coating of some of the damaged optic nerve fibers was not fully degenerated and was therefore more easily restored following folate supplementation, whereas the damage was complete for other fibers such that myelin regeneration, and the consequent functional recovery, might

have been more difficult in the latter case. Having said this, because we did not perform a systematic longitudinal study, we are not in the position to exclude that the recovery would have progressed further after additional months of treatment, in line with data in the literature indicating very slow recovery in this kind of disease (e.g., see Refs. 5–9).

The visual deficits associated with optic nerve demyelination were established by means of the systematic psychophysical assessment of CS, which allowed us to ascertain compromised visual performance in the affected monkeys for visual stimuli presented at low and intermediate contrast levels. As long acknowledged (e.g., see Refs. 37, 38), CS assessments are an important tool for uncovering abnormalities linked to optic neuritis, which instead might not have an impact on less sensitive visual tests, such as the Snellen test for visual acuity. The described CS reduction is well compatible with a distinct damage in signal transmission along the magnocellular pathway of the visual system,[39] although we are not in the position to exclude that an analogous damage affected transmission along the parvocellular pathway.

New to the field, besides behavioral testing and the standard ophthalmological examination, we provided a systematic examination of the neuronal correlates of the disease at the level of the cortical visual system. In particular, we measured single-cell spiking activity at the level of visual area V4d, a mid-tier cortical site of the ventral visual stream,[19,31,32] in response to stimuli of varying luminance contrast. As a result of folic acid deficient optic neuritis, neuronal CRFs were found to be substantially affected by a strong reduction of spiking activity in response to low and intermediate contrast levels, resulting in a critical loss of neuronal CS, nicely paralleling behavioral data. In addition, intertrial variability in neuronal activity measured for low and intermediate contrast was markedly increased, likely reflecting a substantial reduction in the strength of the incoming visual input (e.g., see Ref. 34). Finally, we also found the latency of neuronal responses to be profoundly affected by the disease with marked slowing in neuronal activation even in response to high-contrast stimuli, which might well reflect a decrease in conduction velocity due to demyelination (e.g., see Ref. 40). This finding is in line with some reports of delayed visual activity following demyelination, as measured by an increased latency of visual-evoked potentials, in the absence of amplitude reductions (e.g., Refs. 41–44). It will be of great interest to confirm (and extend) the described electrophysiological signatures of the pathology in future studies with single-unit recordings from other regions of the visual system, including at the subcortical level (e.g., from the lateral geniculate nucleus).

Albeit unfeasible in the current research study for several practical and ethical reasons, it also would have been extremely interesting to collect electrophysiological data from area V4d in monkey B after the observed (partial) recovery of function following folate supplementation. Our prediction is that behavioral recovery would have been nicely paralleled by compatible changes in the relevant parameters describing neuronal activity within this cortical area. Mainly, the recovery in neuronal function would have been reflected in a substantial increase in the strength of visually driven activity, as well as in a clear reduction in both across-trial variability in spike trains, and latency of neuronal response. Such changes would have been the expected consequence of a (partially) restored visual drive along the (partially) remyelinated optic nerve fibers.

In sum, reduced, more variable and delayed neuronal activity in V4 following folic acid–deficient optic neuritis likely reflects inefficient transmission of the preserved retinal input through the damaged, demyelinated optic nerve fibers. It has been proposed that low levels of tetrahydrofolate in folic acid–deficient individuals might result in abnormal increases in the concentration of endogenous formate, reflecting insufficient detoxification processes[7]; as a result, serious damage to the optic nerve might arise as a consequence of the known myelinoclastic effect of formic acid.[45,46] Albeit plausible, this functional explanation still awaits systematic confirmation in future research. In fact, although the current research in behaving macaque monkeys has successfully unveiled strong correspondence between clinically evident signs of ocular pathology, behavioral deficits and reduced/delayed cortical activation at relatively high levels of the visual processing hierarchy, further investigation of the detailed neurobiological and molecular mechanisms underlying folate-deficient optic neuritis will likely benefit from case-control studies in the mouse model. The main message here is that it will be no longer possible to overlook a distinctive role of folic acid deficiency in the development of optic neuritis.

Acknowledgments

Supported by the University of Verona, Verona, Italy.

Disclosure: **E. Santandrea**, None; **I. Sani**, None; **G. Morbioli**, None; **D. Multari**, None; **G. Marchini**, None; **L. Chelazzi**, None

References

1. Congdon NG, West KP. Nutrition and the eye. *Curr Opin Ophthalmol*. 1999;10:464–473.
2. Orssaud C, Roche O, Dufier JL. Nutritional optic neuropathies. *J Neurol Sci*. 2007;262:158–164.
3. Shams PN, Plant GT. Optic neuritis: a review. *Int MS J*. 2009; 16:82–89.
4. Rizzo JF III. Adenosine triphosphate deficiency: a genre of optic neuropathy. *Neurology*. 1995;45:11–16.
5. Chisholm IA. Serum cobalamin and folate in the optic neuropathy associated with tobacco smoking. *Can J Ophthal*. 1978;13:105–109.
6. Knox DL, Chen MF, Guilarte TR, Dang CV, Bumette J. Nutritional amblyopia: folic acid, vitamin B-12, and other vitamins. *Retina*. 1982;2:288–293.
7. Golnik KC, Schaible ER. Folate-responsive optic neuropathy. *J Neuroophtalmol*. 1994;14:163–169.
8. Hsu CT, Miller NR, Wray ML. Optic neuropathy from folic acid deficiency without alcohol abuse. *Opthalmologica*. 2002;216: 65–67.
9. de Silva P, Jayamanne G, Bolton R. Folic acid deficiency optic neuropathy: a case report. *J Med Case Rep*. 2008;2:299.
10. Kesler A, Pianka P. Toxic optic neuropathy. *Curr Neurol Neurosci Rep*. 2003;3:10–14.
11. Krohn PL, Oxnard CE, Chalmers JN. Vitamin B12 in the serum of the rhesus monkey. *Nature*. 1963;197:186.
12. Wadia NH, Desai MM, Quadros EV, Dastur DK. Role of vegetarianism, smoking, and hydroxocobalamin in optic neuritis. *Br Med J*. 1972;3:264–267.
13. Chester EM, Agamanolis DP, Harris JW, Victor M, Hines JD, Kark JA. Optic atrophy in experimental vitamin B12 deficiency in monkeys. *Acta Neurol Scand*. 1980;61:9–26.
14. Brontë-Stewart J, Pettigrew AR, Foulds WS. Toxic optic neuropathy and its experimental production. *Trans Ophthalmol Soc UK*. 1976;96:355–358.
15. Rizzo JF III, Lessell S. Tobacco amblyopia. *Am J Ophthalmol*. 1993;116:84–87.
16. Robinson DA. A method of measuring eye movements using a scleral search coil in a magnetic field. *IEEE Trans Biomed Eng*. 1963;101:131–145.

17. Mirabella G, Bertini G, Samengo I, et al. Neurons in area V4 of the macaque translate attended visual features into behaviorally relevant categories. *Neuron*. 2007;54:303–318.
18. Barlow HB, Blakemore C, Pettigrew JD. The neural mechanism of binocular depth discrimination. *J Physiol*. 1967;193:327–342.
19. Desimone R, Schein SJ. Visual properties of neurons in area V4 of the macaque: sensitivity to stimulus form. *J Neurophysiol*. 1987;57:835–868.
20. Judge SJ, Richmond BJ, Chu FC. Implantation of magnetic search coils for measurement of eye position: an improved method. *Vision Res*. 1980;20:535–538.
21. Albrecht DG, Hamilton DB. Striate cortex of monkey and cat: contrast response function. *J Neurophysiol*. 1982;48:217–237.
22. Pelli DG, Bex P. Measuring contrast sensitivity. *Vis Res*. 2013;90:10–14.
23. Gawne TJ, Kjaer TW, Richmond BJ. Latency: another potential code for feature binding in striate cortex. *J Neurophysiol*. 1996;76:1356–1360.
24. Lee J, Williford T, Maunsell JH. Spatial attention and the latency of neuronal responses in macaque area V4. *J Neurosci*. 2007;27:9632–9637.
25. Sani I, Santandrea E, Golzar A, Morrone MC, Chelazzi L. Selective tuning for contrast in macaque area V4. *J Neurosci*. 2013;33:18583–18596.
26. Sani I, Santandrea E, Morrone MC, Chelazzi L. Temporally evolving gain mechanisms of attention in macaque area V4. *J Neurophysiol*. 2017;118:964–985.
27. Kiorpes L, Kiper DC. Development of contrast sensitivity across the visual field in macaque monkeys (*Macaca nemestrina*). *Vision Res*. 1996;36:239–247.
28. Nicolosi RJ, Hunt RD. Dietary allowances for nutrients in nonhuman primates. In: Hayes KC, ed. *Primates in Nutritional Research*. New York: Academic Press; 1979:11–37.
29. Venter FS, Cloete H, Seier JV, Faber M, Fincham JE. Folic acid and vitamin B_{12} status of vervet monkeys used for nutritional research. *Lab Anim*. 1993;27:59–64.
30. National Research Council. *Nutrient Requirements of Nonhuman Primates*. 2nd ed. Washington, DC: The National Academies Press: 2003.
31. Schein SJ, Desimone R. Spectral properties of V4 neurons in the macaque. *J Neurosci*. 1990;10:3369–3389.
32. Roe AW, Chelazzi L, Connor CE, et al. Toward a unified theory of visual area V4. *Neuron*. 2012;74:12–29.
33. Cheng K, Hasegawa T, Saleem KS, Tanaka K. Comparison of neuronal selectivity for stimulus speed, length, and contrast in the prestriate visual cortical areas V4 and MT of the macaque monkey. *J Neurophysiol*. 1994;71:2269–2280.
34. Mitchell JF, Sundberg KA, Reynolds JH. Differential attention-dependent response modulation across cell classes in macaque visual area V4. *Neuron*. 2007;55:131–141.
35. Albrecht DG. Visual cortex neurons in monkey and cat: effect of contrast on the spatial and temporal phase transfer functions. *Vis Neurosci*. 1995;12:1191–1210.
36. Sundberg KA, Mitchell JF, Gawne TJ, Reynolds JH. Attention influences single unit and local field potential response latencies in visual cortical area V4. *J Neurosci*. 2012;32:16040–16050.
37. Regan D, Silver R, Murray TJ. Visual acuity and contrast sensitivity in multiple sclerosis: hidden visual loss. *Brain*. 1977;100:563–573.
38. Zimmern RL, Campbell FW, Wilkinson IMS. Subtle disturbances of vision after optic neuritis elicited by studying contrast sensitivity. *J Neurol*. 1979;42:407–412.
39. Cao D, Zele AJ, Pokorny J, et al. Funtional loss in the magnocellular and parvocellular pathways in patients with optic neuritis. *Invest Ophthalmol Vis Sci*. 2011;52:8900–8907.
40. Waxman SG. Conduction in myelinated, unmyelinated, and demyelinated fibers. *Arch Neurol*. 1977;34:585–589.
41. Halliday AM, McDonald WI, Mushin J. Delayed pattern visual evoked responses in optic neuritis in relation to visual acuity. *Trans Ophthalmol Soc UK*. 1973;93:315–324.
42. Plant GT. Transient visually evoked potentials to sinusoidal gratings in optic neuritis. *J Neurol Neurosurg Psychiatry*. 1983;46:1125–1133.
43. Burton EV, Greenberg BM, Frohman EM. Optic neuritis: a mechanistic view. *Pathophysiol*. 2011;18:81–92.
44. Holdeman NR, Nguyen T, Tang RA. Demyelinating optic neuritis presenting as a clinically isolated syndrome. *Optometry*. 2012;83:9–18.
45. Martin-Amat G, McMartin KE, Hayreh SS, Hayreh MS, Tephly TR. Methanol poisoning: ocular toxicity produced by formate. *Toxicol Appl Pharmacol*. 1979;45:201–208.
46. Takao H, Doi I, Watanabe T. Serial diffusion-weighted magnetic resonance imaging in methanol intoxication. *J Comput Assist Tomogr*. 2006;30:742–744.

Investigative Ophthalmology & Visual Science